Inorg. Chem. **1987**, *26*, 1529–1535 **1529**

Contribution from the Department of Chemistry,
University of Virginia, Charlottesville, Virginia 22901

Heterobinuclear Adducts of Copper Tetradentate Schiff Bases with Metal Hexafluoroacetylacetonates

Greg A. Brewer and Ekk Sinn*

Received October 21, 1985

A series of heterobinuclear complexes was prepared by the reaction of copper tetradentate Schiff base complexes, Cu(TSB), with metal hexafluoroacetylacetonates, M(hfa)$_2$ (M = Ni(II), Co(II), Fe(II), Mn(II)). The Schiff base ligands, H$_2$((prp)$_2$en) and H$_2$((prp)$_2$pr), were prepared from the condensation of *o*-hydroxypropiophenone, Hprp, with ethylenediamine, en, or 1,3-propylenediamine, pr, respectively. The crystal structures of three of the complexes, Cu((prp)$_2$en)Fe(hfa)$_2$, Cu((prp)$_2$pr)Fe(hfa)$_2$, and Cu((prp)$_2$pr)Co(hfa)$_2$, were determined and refined to *R* values of 6.1, 8.3, and 6.3% for 1107, 2258, and 1411 reflections, respectively. Cu((prp)$_2$en)Fe(hfa)$_2$ crystallizes in $P2_1/c$, $Z = 4$, with $a = 13.576$ (7) Å, $b = 20.365$ (5) Å, $c = 12.606$ (7) Å, and $\beta = 97.70$ (5)°. Cu((prp)$_2$pr)Fe(hfa)$_2$ and Cu((prp)$_2$pr)Co(hfa)$_2$ crystallize in $P\bar{1}$, $Z = 2$, with $a = 11.630$ (4) Å, $b = 12.443$ (6) Å, $c = 13.897$ (4) Å, $\alpha = 90.83$ (5)°, $\beta = 95.26$ (4)°, and $\gamma = 116.19$ (4)° and $a = 11.821$ (3) Å, $b = 12.402$ (5) Å, $c = 13.885$ (6) Å, $\alpha = 91.64$ (3)°, $\beta = 95.64$ (3)°, and $\gamma = 116.75$ (3)°, respectively. The magnetic susceptibilities of all complexes were measured between 4 and 110 K. The strength of antiferromagnetic coupling, *J*, is shown to depend on the angle, Φ, between the O(1)–Cu–O(2) and O(1)–M–O(2) planes and on the Cu–O–M angle. Thus, a 5° increase in Φ in the pr series of Cu–Fe compounds over the value in the en series is accompanied by an increase in the quartet–sextet separation, $-5J$, from 30 to 115 cm^{-1}. This series better models some of the electronic properties of cytochrome oxidase than a wide variety of literature binuclear complexes, and it lends support to a CuOFe center in the enzyme with a metal–metal separation of a little over 3 Å.

Introduction

The interest in heterobinuclear transition-metal complexes has risen sharply in recent years.[1–18] Heterobinuclear complexes have been used as models for the active sites of many enzyme systems.[19] Of particular importance is the respiratory enzyme cytochrome *c* oxidase, which, on the basis of the observation of strong coupling between the metals, has been postulated to contain an Fe(III) linked to a Cu(II).[20,21] Although initial reports favored an imidazolate (Im) fragment as the likely bridge, subsequent work has indicated that the bridge may be an oxygen[22–24] or sulfur atom.[25–27]

Promotion of magnetic coupling via a sulfur bridge is illustrated by Fe(Salen)$_2$S, which resembles Fe(Salen)$_2$O magnetically[28,29] and structurally.[30] The strong Fe–S–Fe and Fe–O–Fe bridges in these complexes each promote strong antiferromagnetic interactions. However, the sulfur-bridged species proposed for cytochrome oxidase has a semicoordinated sulfur, Fe–S = 2.60 Å, with Fe–Cu = 3.75 Å.[27] This is unlikely to promote strong coupling, and a recently synthesized model complex with Fe–S–Cu bridges is reported to be uncoupled.[17] Relatively strong coupling with Im bridging is also observed in homobinuclear complexes, even when pairs of copper(II) ions are held as much as 6 Å apart.[31–34] However, Im-bridged cytochrome oxidase models require such coupling between pairs of dissimilar metals. The appropriate heterobinuclear M–Im–N′ complexes have tended to be either noncoupled or weakly coupled.[14,15,35,36] One apparent exception is an [Fe(Im)Cu](trifluoromethanesulfonate) complex that could not be studied in solution or structurally characterized in the solid-state.[37] O bridges have long been known to produce strong coupling in heterobinuclear systems.[1,3–8]

---

(1) (a) Gruber, S. J.; Harris, C. M.; Sinn, E. *Inorg. Nucl. Chem. Lett.* **1967**, *3*, 495. (b) *Inorg. Chem.* **1968**, *7*, 268. (c) *Inorg. Nucl. Chem. Lett.* **1968**, *3*, 107. (d) *J. Inorg. Nucl. Chem.* **1968**, *30*, 1805.

(2) Harris, C. M.; James, J. M.; Milham, P. J.; Sinn, E. *Inorg. Chim. Acta* **1969**, *3*, 81.

(3) Sinn, E.; Harris, C. N. *Coord. Chem. Rev.* **1969**, *4*, 391.

(4) Kokot, S.; Harris, C. M.; Sinn, E. *Aust. J. Chem.* **1972**, *25*, 45.

(5) O'Bryan, N. B.; Maier, T. O.; Paul, I. C.; Drago, R. S. *J. Am. Chem. Soc.* **1973**, *95*, 6640.

(6) (a) O'Connor, C. J.; Freyberg, D. P.; Sinn, E. *Inorg. Chem.* **1979**, *18*, 1077. (b) Freyberg, D. P. Doctoral Dissertation, 1978.

(7) Castello, U.; Vigato, P. A.; Viladi, M. *Coord. Chem. Rev.* **1977**, *23*, 31.

(8) Selbin, J.; Ganguly, L. *Inorg. Nucl. Chem. Lett.* **1969**, *8*, 815.

(9) Timken, M. D.; Marritt, W. A.; Hendrickson, D. N.; Gagne, R. R.; Sinn, E. *Inorg. Chem.* **1985**, *24*, 4202.

(10) Brewer, G. A.; Sinn, E. *Inorg. Chem.* **1984**, *23*, 2532.

(11) Sinn, E.; Brewer, G. A., paper presented at XXIInd ICCC, Budapest, Hungary, Aug 23–27, 1982. Brewer, G. A.; Sinn, E. *Inorg. Chim. Acta* **1984**, *87*, L41. Brewer, G. A. Thesis, 1982.

(12) Kovacs, D.; Shepherd, R. E. *J. Inorg. Biochem.* **1979**, *10*, 67.

(13) Gunter, M. J.; Berry, K. J.; Murray, K. S. *J. Am. Chem. Soc.* **1984**, *106*, 4227.

(14) Prosperi, T.; Tomlinson, A. A. G. *J. Chem. Soc., Chem. Commun.* **1979**, 196.

(15) Saxton, R. J.; Wilson, L. J. *J. Chem. Soc., Chem. Commun.* **1984**, 359.

(16) Chang, C. K.; Koo, M. S.; Ward, B. *J. Chem. Soc., Chem. Commun.* **1982**, 716.

(17) Schauer, C. K.; Akabori, K.; Elliott, C. M.; Anderson, O. P. *J. Am. Chem. Soc.* **1984**, *106*, 1127.

(18) Landrum, J. T.; Grimmet, D.; Haller, K. J.; Scheidt, W. R.; Reed, C. A. *J. Am. Chem. Soc.* **1981**, *103*, 2640.

(19) Davis, W. M.; Dewan, J. C.; Lippard, S. J. *Inorg. Chem.* **1981**, *20*, 2928.

(20) Palmer, G.; Babcock, G. T.; Vickery, L. E. *Proc. Natl. Acad. Sci. U.S.A.* **1976**, *23*, 2206.

(21) Tweedle, M. F.; Wilson, L. J.; Garcia-Iniguez, L.; Babcock, G. T.; Palmer, G. *J. Biol. Chem.* **1978**, *253*, 8065.

(22) Reed, C. A.; Landrum, J. T. *FEBS Lett.* **1979**, *106*, 265.

(23) Shaw, R. W.; Rif, M. H.; O'Leary, M. H.; Beinert, H. *J. Biol. Chem.* **1980**, *256*, 1105.

(24) Petty, R. H.; Welch, B. R.; Wilson, L. J.; Bottomley, L. A.; Kadish, K. M. *J. Am. Chem. Soc.* **1980**, *102*, 611.

(25) Powers, L.; Chance, B.; Ching, Y.; Angiolillo, P. *Biophys. J.* **1981**, *34*, 465.

(26) Chance, B.; Kumar, C.; Powers, L.; Ching, Y. *Biophys. J.* **1983**, *44*, 353.

(27) Powers, L.; Chance, B. In *EXAFS and Near Edge Structure III*; Hodgson, K. O., Hedman, B., Penner-Hahn, J., Eds. Springer-Verlag: Berlin, 1984.

(28) Mitchell, P. C. H.; Parker, D. A. *J. Inorg. Nucl. Chem.* **1973**, *35*, 1385.

(29) Mitchell, P. C. H.; Parker, D. A. *J. Chem. Soc., Dalton Trans.* **1976**, 1821.

(30) Dorfman, J. R.; Girerd, J.-J.; Simhon, E. D.; Stack, T. D. P.; Holm, R. H. *Inorg. Chem.* **1984**, *23*, 4407.

(31) Kolks, G.; Lippard, S. J.; Waszczak, J. V.; Lilienthal, H. R. *J. Am. Chem. Soc.* **1982**, *104*, 717.

(32) Hendriks, H. M. J.; Birker, P. J. M. W. L.; Verschoor, G. C.; Reedijk, J. *J. Chem. Soc., Dalton Trans.* **1982**, 623.

(33) Haddad, N. S.; Hendrickson, D. N.; Cannady, J. P.; Drago, R. S.; Bieksza, Y. S. *J. Am. Chem. Soc.* **1979**, *101*, 898.

(34) Bencini, A.; Gatteschi, D.; Zanchini, C.; Haasnoot, J. G.; Prins, R.; Reedijk, J. *Inorg. Chem.* **1985**, *24*, 2812.

(35) Landrum, J. T.; Reed, C. A.; Hatano, K.; Scheidt, W. R. *J. Am. Chem. Soc.* **1978**, *100*, 3232.

(36) Sinn, E. In *Biochemical and Inorganic Copper Chemistry*; Karlin, K. D., Zubieta, J., Eds.; Adenine: Guilderland, NY, 1985; see also references cited therein.

(37) Dessens, S. E.; Merrill, C. L.; Saxton, R. J.; Ilaria, R. L., Jr.; Lindsey, J. W.; Wilson, L. J. *J. Am. Chem. Soc.* **1982**, *104*, 4357.

There have been several attempts to prepare synthetic compounds that contain the Fe–Cu couple to compare the magnetism to the model system with that of the enzyme.[10-17,24,37] The strongest coupling observed (quartet–septet separation = 330 cm^{-1}), in heterobinuclear complexes containing oxygen-bridged Cu(II) and Fe(III), is easily strong enough to quench the ESR and model the coupling in cytochrome oxidase.[4,36] Complexes such as **1** are examples of this, but crystal structures have been determined only for analogous binuclears rather than for the complex itself. When interactions are nonzero, Im bridges have generally tended to produce less strongly coupled complexes **2**.[11,36] Values of the coupling constant J ($H = -2JS_1 \cdot S_2$) of around -300 cm^{-1} have generally been associated with cytochrome oxidase, but such magnitudes of the quintet–septet splitting ($S = {}^1/_2 + S = {}^5/_2$ coupling) or of the quartet–sextet splitting ($S = {}^1/_2 + S = 2$ coupling) are required to predict the ESR and magnetic properties.[36]

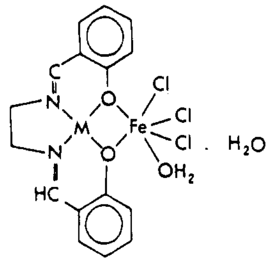

1

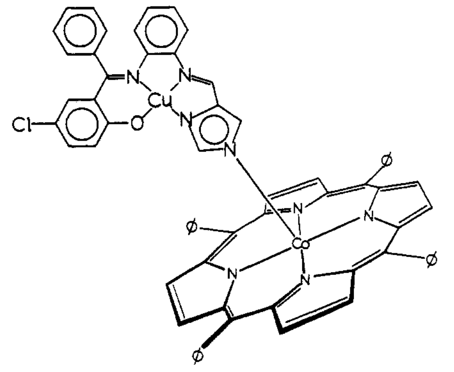

2a

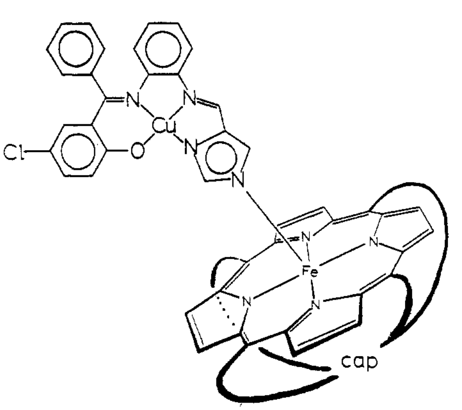

2b

In addition to enzyme modeling, heterobinuclear complexes are of interest in evaluating the factors that contribute to magnetic exchange.[1,36,38,39] A series of closely related heterobinuclear complexes containing two paramagnetic ions will allow the effects of gradual electronic and structural variations to be understood. Heterobinuclear complexes may be symmetric or asymmetric with respect to the metal environment. The preparation of some asymmetric complexes is facilitated by the inherent difference between the two binding sites.

We report the synthesis and characterization of a series of heterobinuclear complexes and the structures of one Cu(II)–Co(II) and two Cu(II)–Fe(II) heterobinuclears. The complexes are formed by the reaction of Cu(TSB) with $M(hfa)_2$ (M = Mn(II), Fe(II), Co(II), Ni(II)). The H_2TSB ligands are the Schiff base condensates of *o*-hydroxypropiophenone with ethylenediamine, $H_2((prp)_2en)$, or with 1,3-propylenediamine, $H_2((prp)_2pr)$.

Experimental Section

General Procedures. $Cu((prp)_2en)$ was prepared as described previously.[6] The $M(hfa)_2$ complexes where M = Mn, Co, and Ni were prepared by standard procedures.[40,41] The method of Buckingham was used to prepare $Fe(hfa)_2$.[42] Elemental analyses were performed by Atlantic Microlabs. Mass spectra were obtained on a conventional electron-impact instrument.

$Cu((prp)_2pr)$. The ligand was prepared by refluxing *o*-hydroxypropiophenone (1.8 g, 0.012 mol) and 1,3-propylenediamine (0.44 g, 0.006 mol) in 50 mL of methanol for 30 min. The solution of the Schiff base was added with stirring to an aqueous solution of copper acetate (1.194 g, 0.006 mol). The green solution yielded a green solid on gentle warming. The product was recrystallized from aqueous methanol.

$Cu((prp)_2pr)M(hfa)_2$. These adducts were prepared by the 1:1 reaction of $Cu((prp)_2pr)$ in dichloromethane with $M(hfa)_2$ in methanol. Crystals of the binuclear product formed in 2–3 days. $Fe(hfa)_2$ must be prepared under nitrogen to prevent oxidation. The solution of the binuclear complex was kept under nitrogen until crystals of the product appeared. The $Cu((prp)_2en)Fe(hfa)_2$ adduct was prepared as described above.

Magnetism. Magnetic susceptibilities (4–110 K) were measured on a SQUID magnetometer. The calibration and method of operation were as described previously.[43,44]

Crystal Data. $Cu((prp)_2en)Fe(hfa)_2$: $CuFeF_{12}O_6N_2C_{30}H_{24}$, mol wt 856, space group $P2_1/c$, $Z = 4$, $a = 13.576$ (7) Å, $b = 20.365$ (5) Å, $c = 12.606$ (7) Å, $\beta = 97.70$ (5)°, $V = 3485$ Å^3, ρ(calcd) = 1.646 g/cm^3, ρ(obsd) = 1.66 g/cm^3, μ(Mo Kα) = 11.9 cm^{-1}, crystal dimensions (distances in millimeters of faces from centroid) (100) 0.28, ($\bar{1}$00) 0.28, (010) 0.035, (0$\bar{1}$0) 0.035, (001) 0.035, (00$\bar{1}$) 0.035; maximum, minimum transmission coefficients 0.92, 0.88.

$Cu((prp)_2pr)Fe(hfa)_2$: $CuFeF_{12}O_6N_2C_{31}H_{26}$, mol wt 870, space group, $P\bar{1}$, $Z = 2$, $a = 11.630$ (4) Å, $b = 12.443$ (6) Å, $c = 13.897$ (4) Å, $\alpha = 90.83$ (5)°, $\beta = 95.26$ (4)°, $\gamma = 116.19$ (4)°, $V = 1794$ Å^3, ρ(calcd) = 1.60 g/cm^3, ρ(obsd) = 1.60 g/cm^3, μ(Mo Kα) = 11.4 cm^{-1}.

$Cu((prp)_2pr)Co(hfa)_2$: $CuCoF_{12}O_6N_2C_{31}H_{26}$, mol wt 873, space group $P\bar{1}$, $Z = 2$, $a = 11.821$ (3) Å, $b = 12.402$ (5) Å, $c = 13.885$ (6) Å, $\alpha = 91.64$ (3)°, $\beta = 95.64$ (3)°, $\gamma = 116.75$ (3)°, $V = 1803$ Å^3, ρ(calcd) = 1.60 g/cm^3, ρ(obsd) = 1.60 g/cm^3.

Data Collection. Cell dimensions and space group data were obtained by standard methods on an Enraf-Nonius four-circle CAD-4 diffractometer using Mo Kα (0.7107 Å) radiation. The θ–2θ scan technique was used at 293 K, as described previously,[45] to record the intensities for all nonequivalent reflections for which $1° \leq 2\theta \leq 48°$. Scan widths were calculated as $(A + B \tan \theta)°$, where A is estimated from the mosaicity of the crystal and B allows for the increase in peak width due to $K\alpha_1$–$K\alpha_2$ splitting. The values of A and B were 0.60 and 0.35°, respectively.

The intensities of four standard reflections showed no greater fluctuations (4%) during data collection than those expected from Poisson statistics. The raw intensity data were corrected for Lorentz–polarization effects and absorption. Of the 4442, 3893, and 3900 independent intensities for $Cu((prp)_2en)Fe(hfa)_2$, $Cu((prp)_2pr)Fe(hfa)_2$, and $Cu((prp)_2pr)Co(hfa)_2$, there were 1107, 2058, and 1411 with $F_o^2 \geq 3\sigma(F_o^2)$, where $\sigma(F_o^2)$ was estimated from counting statistics.[46] These data were used in the final refinement of the structural parameters.

Structure Determination. A three-dimensional Patterson function was used to determine the metal positions in $Cu((prp)_2en)Fe(hfa)_2$ and $Cu((prp)_2pr)Fe(hfa)_2$, which phased the intensity data sufficiently well to permit location of the other non-hydrogen atoms from Fourier synthesis.

---

[38] Tola, P.; Kahn, O.; Chauvel, C.; Coudanne, H. *Nouv. J. Chim.* **1979**, *1*, 467.

[39] Kahn, O.; Charlet, M. F. *Nouv. J. Chim.* **1980**, *4*, 567.

[40] Cotton, F. A.; Holm, R. H. *J. Am. Chem. Soc.* **1960**, *82*, 2979.

[41] Walker, W. R.; Li, N. C. *J. Inorg. Nucl. Chem.* **1965**, *27*, 2255.

[42] Buckingham, D. A.; Gorges, R. C.; Henry, J. T. *Aust. J. Chem.* **1967**, *20*, 281.

[43] O'Connor, C. J.; Sinn, E.; Cukauskas, E. J.; Deaver, B. S. *Inorg. Chim. Acta* **1979**, *32*, 29.

[44] O'Connor, C. J.; Sinn, E.; Deaver, B. S. *J. Chem. Phys.* **1979**, *70*, 5161.

[45] Freyberg, D. P.; Mockler, G. M.; Sinn, E. *J. Chem. Soc., Dalton Trans.* **1976**, 447.

[46] Corfield, P. W. R.; Doedens, R. J.; Ibers, J. A. *Inorg. Chem.* **1967**, *6*, 197.

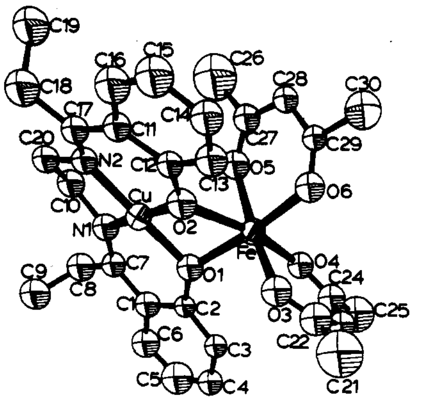

Figure 1. ORTEP diagram of Cu((prp)$_2$en)Fe(hfa)$_2$ with fluorine atoms omitted.

Cu((prp)$_2$pr)Co(hfa)$_2$, is isomorphous with its Cu–Fe analogue, and the coordinates of the latter complex were therefore used as starting parameters in the refinement. Full-matrix least-squares refinement was carried out as previously described.[45] Because of the rather small data sets, anisotropic temperature factors were introduced for only some of the non-hydrogen atoms. Further Fourier difference functions permitted location of the hydrogen atoms, which were included in the refinement for three cycles of least squares and then held fixed. Cu((prp)$_2$en)Fe(hfa)$_2$ converged with $R = 6.1\%$, $R_w = 5.7\%$. Cu((prp)$_2$pr)Fe(hfa)$_2$ and Cu((prp)$_2$pr)Co(hfa)$_2$ converged with $R = 8.3\%$, $R_w = 10.8\%$ and $R = 6.6\%$, $R_w = 6.9\%$, respectively. Tables of observed and calculated structure factors and thermal parameters are available as supplementary material. The principal programs used are as described previously.[45]

Results and Discussion

The synthesis of these adducts is easily accomplished by mixing 1:1 solutions of Cu((prp)$_2$pr) with M(hfa)$_2$ in 50:50 dichloromethane–methanol. The product can be isolated as needles in 24–48 h. In the case of Fe(hfa)$_2$ the solution must be kept under nitrogen to prevent oxidation of the Fe(II) species. In the solid state however, all of the adducts, including those of iron(II), are stable and unreactive toward oxygen, even over a period of several days. The compounds can be characterized quite easily by infrared and electron-impact mass spectroscopy. Although no molecular ion is observed, the mass spectrum gives ions associated with the Cu(TSB) and M(hfa)$_2$ portions of the molecule. As with the previously reported Cu(TSB)M(hfa)$_2$ complexes, the M(hfa)$_2$ peaks are observed at lower temperatures, while the high-temperature mass spectra consist of the Cu(TSB) peaks.

Structures. Table I gives the final positional parameters for the structures reported here. The bond distances and angles are given in Tables II and III. The digits in parentheses in the tables are the standard deviations in the least significant figures quoted and were derived from the inverse matrix in the course of least-squares refinement. The overall structures of these molecules have the copper in a slightly distorted square-planar N_2O_2 environment of the Schiff base and the other metal in a distorted octahedron made up of the four hfa oxygens and the two bridging phenolic oxygens. The structures are similar, with little difference between the molecular diagrams. The important small differences show up as relatively small changes in bond lengths and interplanar angles. The ORTEP diagram and numbering scheme of Cu((prp)$_2$en)Fe(hfa)$_2$ are shown in Figure 1, which illustrates the general geometry of the other complexes. The numbering scheme of the pr complexes is the same except that the carbon atoms between the Schiff base nitrogens are labeled C(1P)–C(3P).

The CuO$_2$Fe bridging unit in the CuFe binuclears is not flat. In Cu((prp)$_2$en)Fe(hfa)$_2$, the CuO$_2$ and O$_2$Fe planes are inclined at an angle $\Phi = 143.9°$ to each other, while in Cu((prp)$_2$pr)Fe(hfa)$_2$, this angle is 148.8°. The Cu environment is slightly distorted toward tetrahedral: in the en complex, the dihedral angle between the two CuON planes is 7.1° instead of the 0 and 45° values expected for planar and tetrahedral geometries, respectively; in the pr complex, the corresponding angle is 9.9°, indicating a similar but slightly greater tetrahedral distortion. The iron atom is distorted from octahedral symmetry. In the en complex, the three equatorial planes of four donor atoms make angles of 89.7, 82.2, and 83.1° to one another instead of the 90° required for a regular octahedron; the corresponding angles in the pr complex are 88.3, 83.2, and 75.1°, again indicating a slightly greater distortion. The hfa ligands in the en complex are bent away from the appropriate equatorial planes, one by 14.3° and one by 17.7°; in the pr complex, they are bent away by 12.0 and 18.0°. The distortion is similar for Cu((prp)$_2$pr)Co(hfa)$_2$: 11.1° for the dihedral angle between the CuON planes, 86.0, 85.3, and 84.8° for the equatorial angles, and 11.7 and 20.3° for the inclination of the hfa rings to the equatorial planes.

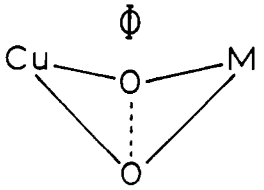

Figure 2. Angle Φ between the CuO$_2$ and O$_2$M planes.

It is interesting to compare the structures of Cu((prp)$_2$en) and Cu((prp)$_2$pr) adducts with those of M(hfa)$_2$ adducts in general. The only chemical difference between the two series is the number of methylene groups between the imine nitrogens of the Schiff base. This minor chemical change produces distortions in the Schiff base that are manifested in the structure of the adducts (Table IV). The change from en to pr widens the N–Cu–N angle by 8.0° and by a scissoring action constricts the O–Cu–O angle by 6.2°. The constriction of the O–Cu–O angle reduces the bite of the Cu(TSB) complex by an average of 0.08 Å, which in turn affects the manner in which it adducts to other species.

The most notable effect of the change in the Cu(TSB) bite angle is to widen the interplanar angle, Φ, between CuO$_2$ and O$_2$M planes of the butterfly-shaped CuO$_2$M center (Figure 2). As can be seen from the data given in Table IV, the interplanar angle widens about 5° with a change from en to pr. This widening of Φ must be attributed to the pinching of the O–Cu–O bite angle, which in turn is caused by the widening of the N–Cu–N angle. Changing the diamine portion of the Cu(TSB) causes a ripple of structural distortions that involve widening the N–Cu–N angle, pinching the O–Cu–O angle, and ultimately an increase in Φ.

Magnetism. J and g values for the complexes were determined from the fit of the magnetic susceptibility to temperature. ESR data would give g for the Cu site without providing information on the other metal. However, the spectra gave only broad peaks, which permit only approximate g values. At low temperature, the solids give ESR spectra for the Cu–Ni and the Cu–Mn complexes, but not for Cu((prp)$_2$pr)Fe(hfa)$_2$ or for the Cu–Co complexes. Cu((prp)$_2$en)Fe(hfa)$_2$ produced a poorly resolved spectrum centered at $g = 2.05$. The absence of an ESR signal is unusual because the slow relaxation of copper(II) tends to give an ESR signal at all temperatures. The dipolar interaction with the proximate other metal of the heteropair presumably speeds up the relaxation time. The conditions that eliminate the ESR spectrum should lead to an observable NMR spectrum: if the relaxation is fast enough on the NMR time scale, the effect of the unpaired electron density should not be visible.[5,47] This was tested for Cu((prp)$_2$pr)Co(hfa)$_2$, which is sufficiently soluble in CDCl$_3$. This shows the ethyl groups cleanly resolved at 3.5 and 1.2 ppm. The ESR of this solution showed only a slight signal centered at $g = 2.0$. A few drops of pyridine were added to this solution to break up the adduct into isolated Cu(hfa)$_2$(py)$_2$ and Cu((prp)$_2$pr) molecules. The resulting ESR spectrum showed a copper signal enhanced by a factor of 100. The NMR spectrum still showed the ethyl pattern, but at reduced intensity. This shows that the binuclear material exists in noncoordinating solvents but is at least partially broken up when small amounts of strong Lewis base are added. This technique is used estimate intermetallic distances,[47] though here this is known from the X-ray data. Only

---

(47) Dei, A.; Gatteschi, D.; Piergentili, E. *Inorg. Chem.* **1979**, *18*, 89.

Table I. Positional Parameters and Esd's

	x	*y*	*z*		*x*	*y*	*z*
(a) Cu((prp)$_2$pr)Co(hfa)$_2$							
Cu	−0.0118 (3)	0.0631 (3)	0.2218 (2)	C(1)	0.068 (2)	−0.082 (2)	0.379 (2)
Co	0.2561 (4)	0.2681 (3)	0.2667 (2)	C(2)	0.166 (2)	0.008 (2)	0.341 (2)
F(1)	0.707 (2)	0.394 (2)	0.165 (2)	C(3)	0.290 (2)	0.019 (2)	0.349 (2)
F(2)	0.548 (2)	0.287 (3)	0.072 (1)	C(4)	0.314 (3)	−0.075 (3)	0.394 (2)
F(3)	0.629 (2)	0.214 (2)	0.155 (2)	C(5)	0.212 (3)	−0.165 (3)	0.426 (2)
F(4)	0.536 (2)	0.422 (1)	0.555 (1)	C(6)	0.093 (3)	−0.180 (3)	0.428 (2)
F(5)	0.524 (2)	0.248 (1)	0.540 (1)	C(7)	−0.066 (2)	−0.099 (2)	0.380 (2)
F(6)	0.690 (1)	0.396 (2)	0.504 (1)	C(8)	−0.154 (2)	−0.189 (2)	0.449 (2)
F(7)	−0.099 (2)	0.321 (2)	0.325 (2)	C(9)	−0.229 (2)	−0.316 (2)	0.400 (2)
F(8)	−0.013 (2)	0.508 (1)	0.333 (1)	C(11)	−0.023 (2)	0.127 (2)	−0.002 (2)
F(9)	0.019 (2)	0.416 (2)	0.445 (1)	C(12)	0.096 (2)	0.196 (2)	0.054 (2)
F(10)	0.507 (2)	0.663 (2)	0.195 (2)	C(13)	0.208 (3)	0.278 (2)	0.023 (2)
F(11)	0.354 (3)	0.639 (2)	0.107 (1)	C(14)	0.208 (3)	0.300 (2)	−0.083 (2)
F(12)	0.400 (3)	0.733 (2)	0.228 (2)	C(15)	0.085 (2)	0.230 (2)	−0.139 (2)
O(1)	0.148 (2)	0.101 (1)	0.302 (1)	C(16)	−0.019 (2)	0.153 (2)	−0.105 (2)
O(2)	0.107 (2)	0.180 (1)	0.154 (1)	C(17)	−0.139 (2)	0.053 (2)	0.025 (2)
O(3)	0.387 (1)	0.245 (1)	0.197 (1)	C(18)	−0.264 (3)	−0.011 (2)	−0.046 (2)
O(4)	0.378 (1)	0.302 (1)	0.397 (1)	C(19)	−0.326 (2)	0.075 (2)	−0.071 (2)
O(5)	0.128 (2)	0.313 (1)	0.323 (1)	C(21)	0.604 (3)	0.306 (3)	0.157 (3)
O(6)	0.343 (2)	0.441 (1)	0.224 (1)	C(22)	0.507 (2)	0.295 (2)	0.224 (2)
OX	0.057 (2)	0.602 (2)	0.953 (2)	C(23)	0.573 (2)	0.341 (2)	0.326 (2)
N(1)	−0.118 (2)	−0.040 (2)	0.322 (1)	C(24)	0.489 (2)	0.328 (2)	0.395 (2)
N(2)	−0.161 (2)	0.026 (2)	0.124 (2)	C(25)	0.570 (2)	0.357 (2)	0.506 (2)
C(1P)	−0.250 (2)	−0.060 (2)	0.334 (2)	C(26)	0.008 (3)	0.412 (3)	0.349 (2)
C(2P)	−0.288 (3)	0.013 (2)	0.259 (2)	C(27)	0.119 (2)	0.412 (2)	0.311 (2)
C(3P)	−0.287 (2)	−0.036 (2)	0.155 (2)	C(28)	0.195 (2)	0.509 (2)	0.262 (2)
				C(29)	0.304 (2)	0.516 (2)	0.229 (2)
				C(30)	0.390 (3)	0.638 (3)	0.190 (2)
(b) Cu((prp)$_2$pr)Fe(hfa)$_2$							
Cu	−0.0136 (4)	0.0612 (3)	0.2198 (2)	C(1)	0.060 (3)	−0.084 (2)	0.382 (2)
Fe	0.2541 (5)	0.2721 (4)	0.2681 (3)	C(2)	0.169 (3)	0.005 (3)	0.343 (2)
F(1)	0.706 (3)	0.393 (3)	0.160 (2)	C(3)	0.282 (3)	0.015 (3)	0.349 (2)
F(2)	0.545 (3)	0.280 (6)	0.070 (2)	C(4)	0.320 (4)	−0.069 (4)	0.388 (3)
F(3)	0.642 (4)	0.222 (3)	0.153 (2)	C(5)	0.205 (4)	−0.162 (4)	0.424 (3)
F(4)	0.542 (2)	0.426 (2)	0.554 (1)	C(6)	0.091 (3)	−0.172 (3)	0.427 (3)
F(5)	0.533 (3)	0.251 (2)	0.541 (1)	C(7)	−0.061 (3)	−0.098 (3)	0.380 (2)
F(6)	0.698 (2)	0.394 (2)	0.499 (1)	C(8)	−0.154 (3)	−0.182 (3)	0.452 (2)
F(7)	−0.105 (3)	0.320 (3)	0.322 (3)	C(9)	−0.234 (3)	−0.311 (3)	0.395 (3)
F(8)	−0.021 (3)	0.505 (2)	0.340 (2)	C(11)	−0.019 (2)	0.130 (2)	−0.003 (2)
F(9)	0.012 (4)	0.410 (3)	0.446 (2)	C(12)	0.088 (3)	0.197 (3)	0.048 (2)
F(10)	0.508 (3)	0.666 (2)	0.201 (2)	C(13)	0.212 (3)	0.275 (3)	0.019 (2)
F(11)	0.355 (5)	0.641 (2)	0.107 (1)	C(14)	0.209 (3)	0.295 (3)	−0.084 (3)
F(12)	0.398 (4)	0.739 (2)	0.236 (2)	C(15)	0.088 (3)	0.231 (3)	−0.140 (3)
O(1)	0.146 (2)	0.093 (2)	0.295 (1)	C(16)	−0.017 (3)	0.149 (3)	−0.111 (3)
O(2)	0.112 (2)	0.183 (2)	0.152 (1)	C(17)	−0.140 (3)	0.053 (3)	0.020 (2)
O(3)	0.388 (2)	0.251 (1)	0.199 (1)	C(18)	−0.265 (3)	−0.007 (3)	−0.051 (2)
O(4)	0.384 (2)	0.306 (1)	0.394 (1)	C(19)	−0.331 (3)	0.073 (3)	−0.065 (3)
O(5)	0.132 (2)	0.316 (2)	0.320 (1)	C(21)	0.596 (4)	0.299 (4)	0.151 (3)
O(6)	0.342 (2)	0.447 (2)	0.228 (1)	C(22)	0.496 (3)	0.290 (3)	0.217 (2)
OX	0.053 (3)	0.610 (3)	0.948 (2)	C(23)	0.575 (3)	0.331 (3)	0.324 (2)
N(1)	−0.114 (2)	−0.043 (2)	0.327 (2)	C(24)	0.490 (2)	0.330 (2)	0.393 (2)
N(2)	−0.160 (2)	0.023 (2)	0.125 (2)	C(25)	0.579 (3)	0.359 (3)	0.503 (2)
C(1P)	−0.251 (3)	−0.056 (3)	0.329 (2)	C(26)	0.007 (3)	0.413 (3)	0.346 (3)
C(2P)	−0.289 (4)	0.020 (3)	0.255 (3)	C(27)	0.109 (3)	0.405 (2)	0.315 (2)
C(3P)	−0.288 (3)	−0.037 (3)	0.154 (2)	C(28)	0.196 (3)	0.517 (3)	0.267 (2)
				C(29)	0.300 (2)	0.517 (2)	0.233 (2)
				C(30)	0.393 (3)	0.644 (3)	0.192 (2)
(c) Cu((prp)$_2$en)Fe(hfa)$_2$							
Cu	0.2853 (3)	0.5124 (2)	0.4714 (3)	F(10)	0.436 (2)	0.5997 (16)	0.004 (3)
Fe	0.2370 (3)	0.4832 (2)	0.2367 (3)	F(11)	0.314 (2)	0.5490 (15)	−0.095 (2)
F(1)	0.404 (2)	0.2975 (14)	0.136 (2)	F(12)	0.314 (2)	0.6527 (15)	−0.072 (2)
F(2)	0.293 (2)	0.2515 (16)	0.061 (2)	F(10′)	0.388 (2)	0.6564 (13)	−0.014 (2)
F(3)	0.351 (3)	0.3427 (21)	−0.026 (3)	F(11′)	0.278 (2)	0.5932 (16)	−0.105 (2)
F(1′)	0.296 (2)	0.2756 (14)	−0.013 (3)	F(12′)	0.411 (2)	0.5514 (14)	−0.031 (2)
F(2′)	0.417 (3)	0.3307 (18)	0.081 (3)	O(1)	0.207 (1)	0.4497 (8)	0.387 (1)
F(3′)	0.328 (3)	0.2627 (22)	0.168 (3)	O(2)	0.361 (1)	0.5096 (8)	0.358 (1)
F(4)	−0.027 (1)	0.3502 (9)	−0.037 (1)	O(3)	0.296 (1)	0.3973 (8)	0.188 (1)
F(5)	−0.069 (1)	0.4405 (8)	0.022 (1)	O(4)	0.102 (1)	0.4497 (8)	0.157 (1)
F(6)	−0.066 (1)	0.3603 (9)	0.115 (1)	O(5)	0.191 (1)	0.5791 (0)	0.270 (1)
F(7)	0.231 (1)	0.7432 (10)	0.259 (2)	O(6)	0.281 (1)	0.5239 (8)	0.102 (1)
F(8)	0.222 (1)	0.6890 (9)	0.391 (1)	N(1)	0.189 (1)	0.5184 (10)	0.575 (1)
F(9)	0.101 (1)	0.7018 (9)	0.282 (1)	N(2)	0.366 (1)	0.5766 (9)	0.552 (1)

Table I (Continued)

	x	*y*	*z*
C(1)	0.098 (2)	0.419 (1)	0.519 (2)
C(2)	0.142 (2)	0.406 (1)	0.421 (2)
C(3)	0.122 (2)	0.350 (1)	0.362 (2)
C(4)	0.056 (2)	0.305 (1)	0.396 (2)
C(5)	0.012 (2)	0.318 (2)	0.485 (2)
C(6)	0.034 (2)	0.371 (1)	0.549 (2)
C(7)	0.117 (2)	0.477 (1)	0.586 (2)
C(8)	0.057 (2)	0.486 (1)	0.683 (2)
C(9)	0.104 (2)	0.450 (1)	0.784 (2)
C(10)	0.212 (2)	0.578 (1)	0.636 (2)
C(11)	0.494 (2)	0.586 (1)	0.441 (2)
C(12)	0.448 (2)	0.544 (1)	0.355 (2)
C(13)	0.491 (2)	0.535 (1)	0.263 (2)
C(14)	0.580 (2)	0.565 (1)	0.247 (2)
C(15)	0.628 (2)	0.606 (1)	0.327 (2)
C(16)	0.587 (2)	0.612 (1)	0.416 (2)
C(17)	0.450 (2)	0.598 (1)	0.539 (2)
C(18)	0.510 (2)	0.641 (1)	0.617 (2)
C(19)	0.484 (2)	0.715 (1)	0.597 (2)
C(20)	0.322 (2)	0.593 (1)	0.650 (2)
C(21)	0.327 (3)	0.309 (2)	0.063 (3)
C(22)	0.260 (2)	0.361 (1)	0.115 (2)
C(23)	0.160 (2)	0.359 (1)	0.069 (2)
C(24)	0.090 (2)	0.402 (1)	0.094 (2)
C(25)	−0.017 (2)	0.387 (2)	0.049 (2)
C(26)	0.196 (3)	0.693 (2)	0.296 (3)
C(27)	0.223 (2)	0.631 (1)	0.230 (2)
C(28)	0.266 (2)	0.639 (1)	0.139 (2)
C(29)	0.294 (2)	0.582 (1)	0.083 (2)
C(30)	0.342 (2)	0.598 (1)	−0.023 (2)

Table II. Bond Distances (Å) for Cu(TSB)M$(hfa)_2$ Adducts

bond	Cu($(prp)_2$pr)-Co$(hfa)_2$	Cu($(prp)_2$pr)-Fe$(hfa)_2$	Cu($(prp)_2$en)-Fe$(hfa)_2$
Cu–O(1)	1.95 (1)	1.918 (11)	1.89 (1)
Cu–O(2)	1.87 (1)	1.907 (9)	1.87 (1)
Cu–N(1)	2.04 (1)	2.077 (12)	1.97 (1)
Cu–N(2)	1.99 (2)	1.933 (10)	1.91 (1)
M–O(1)	1.99 (1)	2.076 (9)	2.11 (1)
M–O(2)	2.09 (1)	2.096 (13)	2.18 (1)
M–O(3)	2.02 (1)	2.009 (11)	2.05 (1)
M–O(4)	2.10 (1)	2.113 (10)	2.08 (1)
M–O(5)	2.05 (1)	1.922 (12)	2.11 (1)
M–O(6)	2.05 (1)	2.063 (10)	2.04 (1)

Table III. Bond Angles (deg) for Cu(TSB)M$(hfa)_2$ Complexes

angle	Cu($(prp)_2$pr)-Co$(hfa)_2$	Cu($(prp)_2$pr)-Fe$(hfa)_2$	Cu($(prp)_2$en)-Fe$(hfa)_2$
O(1)–Cu–O(2)	78.2 (5)	76.6 (6)	83.0 (5)
O(1)–Cu–N(1)	92.3 (6)	90.0 (5)	92.1 (5)
O(1)–Cu–N(2)	171.7 (7)	169.5 (6)	178.1 (6)
O(2)–Cu–N(1)	167.4 (5)	163.6 (6)	171.5 (5)
O(2)–Cu–N(2)	95.4 (6)	97.4 (6)	95.3 (5)
N(1)–Cu–N(2)	94.8 (7)	97.2 (4)	89.5 (6)
O(1)–M–O(2)	72.2 (4)	69.3 (4)	70.9 (4)
O(1)–M–O(3)	101.6 (5)	97.2 (4)	97.2 (4)
O(1)–M–O(4)	89.8 (4)	93.4 (4)	93.5 (4)
O(1)–M–O(5)	86.2 (5)	91.5 (5)	91.3 (4)
O(1)–M–O(6)	171.9 (5)	172.5 (4)	172.1 (5)
O(2)–M–O(3)	94.5 (5)	91.4 (5)	97.3 (4)
O(2)–M–O(4)	162.0 (5)	161.8 (5)	164.4 (4)
O(2)–M–O(5)	83.6 (5)	87.1 (5)	81.8 (4)
O(2)–M–O(6)	101.9 (4)	103.6 (4)	101.5 (4)
O(3)–M–O(4)	87.8 (5)	85.4 (4)	85.8 (5)
O(3)–M–O(5)	171.1 (4)	170.0 (4)	170.7 (5)
O(3)–M–O(6)	84.1 (5)	85.1 (5)	85.9 (5)
O(4)–M–O(5)	96.6 (5)	99.0 (4)	97.6 (4)
O(4)–M–O(6)	96.1 (4)	94.0 (4)	94.0 (4)
O(5)–M–O(6)	87.7 (5)	85.6 (5)	85.2 (5)
Cu–O(1)–M	100.3 (5)	100.1 (4)	97.0 (5)
Cu–O(1)–C(2)	119 (1)	123.5 (9)	127 (1)
M–O(1)–C(2)	138 (1)	136.2 (9)	135 (1)
Cu–O(2)–M	99.5 (5)	99.8 (4)	95.2 (5)
Cu–O(2)–C(12)	128 (1)	121.9 (9)	125 (1)
M–O(2)–C(12)	133 (1)	138.2 (10)	133.5 (9)
M–O(3)–C(22)	126 (1)	130.9 (10)	128 (1)
M–O(4)–C(24)	121 (1)	123.6 (8)	126 (1)
M–O(5)–C(27)	126 (1)	134.6 (11)	124 (1)
M–O(6)–C(29)	126 (1)	125.9 (11)	129 (1)
Cu–N(1)–C(7)	118 (1)	118.1 (13)	127 (1)
Cu–N(1)–C(1P)	124 (1)	115.2 (9)	...
Cu–N(1)–C(10)	...	...	107 (1)
Cu–N(2)–C(17)	118 (1)	120.1 (12)	130 (1)
Cu–N(2)–C(3P)	117 (1)	119.2 (9)	...
Cu–N(2)–C(20)	...	...	109 (1)

Table IV. Structural Comparison of Cu($(prp)_2$en)- and Cu($(prp)_2$pr)M$(hfa)_2$ Complexes (Bond Distances in Å; Bond Angles in deg)

	en			pr		
	Cu[a]	Co[a]	Fe	Cu[b]	Co	Fe
O(1)–Cu–O(2)	85.1	83.8	83.0	80.6	78.2	74.6
O(1)–O(2)	2.56	2.52	2.49	2.47	2.41	2.43
N(1)–Cu–N(2)	88.0	88.9	89.5	100.7	94.8	94.9
N(1)–N(2)	2.69	2.69	2.74	3.01	2.96	3.03
Cu–M	3.03	2.96	3.00	3.07	3.03	3.20
Φ	143.9	143.5	143.9	148.3	150.0	148.8
Cu–O(1)–M	101.7	96.8	97.0	103.4	100.3	100.5
Cu–O(2)–M	89.4	92.9	95.4	94.5	99.5	99.8
M–O(1)	2.002	2.067	2.110	1.969	1.993	2.064
M–O(2)	2.400	2.178	2.182	2.286	2.092	2.174
M–O(4)	1.976	2.067	2.044	1.973	2.051	2.045
M–O(6)	2.210	2.082	2.077	2.197	2.102	2.235
M–O(3)	1.971	2.041	2.051	1.995	2.019	1.942
M–O(5)	1.991	2.058	2.110	2.028	2.048	1.874

[a] See ref 6. [b] Brewer, G.; Rowe, T.; Sinn, E., submitted for publication in *Inorg. Chem.*

dilute single-crystal ESR measurements would provide more useful information here.

When the ligands hold two paramagnetic metal atoms near enough to each other to interact magnetically, their spins will be coupled parallel (ferromagnetic) or antiparallel (antiferromagnetic). If the individual ground states can be treated as approximately spherically symmetrical, we can use the spin-only Heisenberg Hamiltonian. For heterobinuclear complexes containing copper, this is $\mathcal{H} = -2J\mathbf{S}_{Cu}\cdot\mathbf{S}$, where the spin quantum number **S** applies to the metal M. This enables us to obtain a general equation for copper heterobinuclears:[36]

$$\chi = \frac{Ng^2\beta^2(2S+1)}{6kT}\,\frac{S(S-{}^1\!/_2)x + (S+1)(S+{}^3\!/_2)}{Sx+S+1} \qquad (1)$$

$$x = e^{-J(2S+1)/kT}$$

This assumes equal *g* values for the two metals, which is often a good representation of reality.[6,12,20,21] When this approximation is not good, we use g_1 and g_2 for the metals Cu and M, to obtain the general equation

$$\chi = N\beta^2\left\{\left[(S+1)(2S+3)(2Sg_1+g_2)^2 + \frac{8}{y}S(S+1)\times (g_1-g_2)^2\right]e^y + S(2S-1)[2(S+1)(g_1-g_2)^2] - \frac{8}{y}S(S+1)(g_1-g_2)^2\right\}\bigg/\{12(2S+1)kT[(S+1)e^y+S]\} \qquad (2)$$

$$y = (2S+1)J/kT$$

Thus, for a d^5–d^9 binuclear, e.g. Fe(III)–Cu(II) or Mn(II)–Cu(II)

$$\chi = \frac{N\beta^2}{18kT}\left\{\left[14(5g_1+g_2)^2 + \frac{35}{y}(g_1-g_2)^2\right]e^y + 5(7g_1-g_2)^2 - \frac{35}{y}(g_1-g_2)^2\right\}\bigg/(7e^y+5) \qquad (3)$$

$$y = 6J/kT$$

For a d^8–d^9 binuclear, e.g. Ni(II)–Cu(II)

$$\chi = \frac{N\beta^2}{18kT}\left\{\left[10(2g_1 + g_2)^2 + \frac{16}{y}(g_1 - g_2)\right]e^y + (4g_1 - g_2) - \frac{16}{y}(g_1 - g_2)^2\right\} \Big/ (4e^y + 2) \quad (4)$$

$$y = 3J/kT$$

The magnetic moments of the $Cu(TSB)M(hfa)_2$ adducts in the 4–110 K temperature region show considerable variation with temperature due to antiferromagnetic exchange between the metals. At the lowest temperatures, the moment is given by $\mu = g[S_T(S_T + 1)]^{1/2}$ where $S_T = S - {}^1/_2$. The g value here is a weighted average for M and Cu. The upper limit of the moment for a Cu(II)–M(II) pair, assuming no coupling, is $\mu = [S_2(S_2 + 1) + {}^3/_4]^{1/2}$.

The data could be better fitted to the theoretical equation when the g values for the two metals are allowed to vary independently, but this raises a risk of overparametrizing the model without independent determination of the g values, such as by ESR. In any case, the optimal J values were little affected by whether the g values are independent or not. The data for the Cu(II)–Ni(II) (Figure 3) system were subjected to a least-squares fit of the theoretical equation resulting from eq 4 when $g = g_1 = g_2$[48,49]

$$\chi = Ng^2\beta^2(10e^y + 1)/[2kT(2 + 4e^y)] + \text{TIP}$$

where TIP is the temperature-independent paramagnetism. The low-temperature moment of this compound of 1.97 μ_B corresponds well with the expected value for a $S = {}^1/_2$ system. Analysis of this compound yielded $g = 2.31$, $-J = 42$ cm^{-1}, and TIP = 140 × 10^{-6} cgsu.

The low-temperature value of the magnetic moment of the Cu(II)–Co(II) complex (Figure 4), 1.20 μ_B, is considerably below the spin-only value of 2.82 μ_B. The deviation is due to spin–orbit coupling and is associated with octahedral cobalt(II), $^4T_1$. The net effect of the spin–orbit coupling here is to reduce the magnetic moment below the spin-only value. Thus, at the lowest temperatures, the effective spin of the Co(II) is ${}^1/_2$. A way to explicitly correct for this phenomenon is the incorporation of the spin–orbit coupling term, $-\lambda \mathbf{L}_{Co} \cdot \mathbf{S}_{Co}$, in the Hamiltonian and diagonalization of a 24 × 24 matrix.[50] However, it is not appropriate for a significantly distorted octahedron that splits the $^4T_1$ state as in the present case. A more approximate and simpler method recently employed for another Cu(II)–Co(II) system[51] includes isotropic exchange, zero-field splitting, and a Curie–Weiss parameter, Θ, in the Hamiltonian. The Co(II)–Cu(II) system was analyzed by the method of Lambert, Spiro, and Gagne, and Hendrickson[51] and yielded $-J = 15$ cm^{-1}, $D = -7.2$ cm^{-1}, $\Theta = -0.58$ and $g = 2.17$. Similar analysis, without the Curie–Weiss parameter, yields $-J = 23$ cm^{-1}, $g = 2.11$, and $D = -0.55$ cm^{-1} for $Cu((prp)_2pr)Fe(hfa)_2$ (Figure 5). $Cu((prp)_2en)Fe(hfa)_2$ yields $-J = 6.0$ cm^{-1} and $g = 2.04$.

The Cu(II)–Mn(II) system (Figure 6) was analyzed by eq 2 with the g values equal, which leads to the theoretical equation reported previously.[49] The low-temperature moment of 5.05 μ_B is in good agreement for this $S = 2$ ground state. Analysis yields $-J = 15$ cm^{-1} and $g = 2.05$. This corresponds to a quintet–septet separation of 90 cm^{-1} and compares with a value of 79 cm^{-1} for the analogous en complex.

It is not possible to analyze the magnetic data simply in terms of an increasing Cu–O–M angle, ϕ, since the principal metal planes are not coplanar. In fact, the main structural difference between the two series is the widening of the interplanar angle, Φ, in the present pr series compared to that in the en series. The magnetic interactions in the $Cu((prp)_2pr)M(hfa)_2$ series are greater than those exhibited by $Cu((prp)_2en)M(hfa)_2$. This is attributed to the greater superexchange orbital overlap of the copper $d_{x^2-y^2}$ orbital with the M orbitals fostered by the more coplanar arrangement of the metals, the slightly shorter M–O(1) and M–O(2) bonds, and the larger Cu–O–M angles of the pr complexes compared to those of the en series. It is impossible to analytically distinguish between these three effects, without a complete series of intermediate structures, because they occur simultaneously. The increase in the Cu–O–M angle, ϕ, of 3–4° would more than account for the observed increase in coupling based on a correlation of J with ϕ for essentially coplanar Cu(II) species with Cu–O–Cu bridges.[52] However, this correlation is not quantitatively applicable here because of the noncoplanarity and the greater number of exchange pathways available to heterobinuclear complexes.

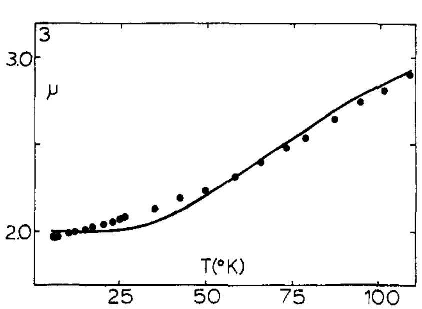

Figure 3. Observed and calculated magnetic data for $Cu((prp)_2pr)Ni(hfa)_2$.

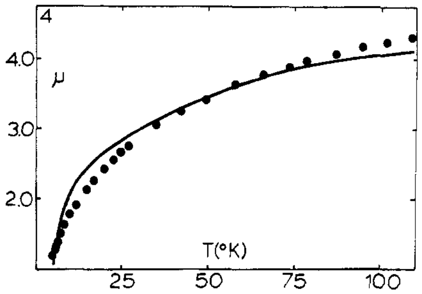

Figure 4. Observed and calculated magnetic data for $Cu((prp)_2pr)Co(hfa)_2$.

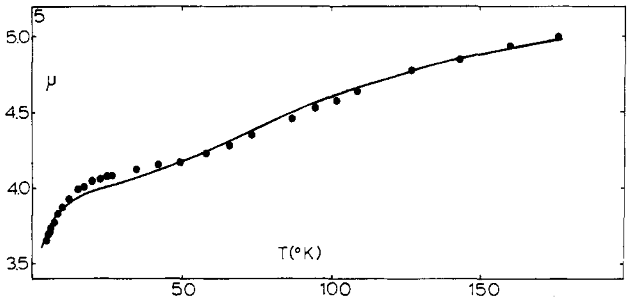

Figure 5. Observed and calculated magnetic data for $Cu((prp)_2pr)Fe(hfa)_2$.

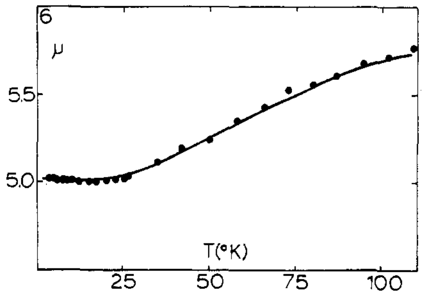

Figure 6. Observed and calculated magnetic data for $Cu((prp)_2pr)Mn(hfa)_2$.

---

[48] Sinn, E. *Coord. Chem. Rev.* **1970**, *5*, 313.

[49] Gruber, S. J.; Harris, C. M.; Sinn, E. *J. Chem. Phys.* **1968**, *18*, 1077.

[50] Kahn, O.; Tola, P. *J. Chem. Phys.* **1979**, *42*, 355.

[51] Lambert, S. L.; Spiro, C. L.; Gagne, R. R.; Hendrickson, D. N. *Inorg. Chem.* **1982**, *21*, 68.

[52] Lewis, D. L.; McGregor, K. T.; Hatfield, W. E.; Hodgson, D. J. *Inorg. Chem.* **1974**, *13*, 1013.

Table V. $-J$ for Selected Cu(II)–M(II) Heterobinuclear Complexes

	metal			
complex type	Ni	Co	Fe	Mn
diformylphenol[a]	103	124	...	30
formylsalicylic acid[b]	75	35	...	22
$\mathrm{Cu((prp)_2en)M(hfa)_2}$[c]	21	11	6[d]	7
$\mathrm{Cu((prp)_2pr)M(hfa)_2}$[d]	42	15	23	15

[a] See ref 50. [b] See ref 56. [c] See ref 6. [d] Present work.

Although these independent structural differences cannot be separated, they are all expected to shift J in the experimentally observed direction.

It is worthwhile to compare the $\mathrm{Cu(TSB)M(hfa)_2}$ heterobinuclear adducts with complexes examined by other workers. One series characterized by Lambert et al. employs a binucleating ligand derived from the condensation of a diamine with 2,6-diformyl-4-methylphenol.[51] The ligand provides a $\mathrm{N_2O_2}$ donor set for each metal. Another series employs a ligand derived from 3-formylsalicylic acid and a diamine.[53] This series is somewhat similar to the present one in that the coordination sites for the two metals are different. This ligand structurally links both metals but does not provide symmetric binding sites as does the ligand derived from 2,6-diformyl-4-methylphenol. The J values of various heterobinuclear complexes are given in Table V. Cu(II)–Fe(II) complexes are formed in the present series but are unreported for the other binucleating ligands. The present series of heterobinuclear complexes offers the least constraint with regard to structural distortions of the Cu–O–M bridge and overall complex geometry. This is due to the fact that a binucleating ligand is not employed and each fragment of the heterobinuclear complex is capable of distortions, within limits, independently of the other. Thus the present series is expected to show a greater amount of individual structural variations than do the other series.

The J values of the other series are consistently greater than those of the $\mathrm{Cu(TSB)M(hfa)_2}$ adducts. This reflects the fact that the binucleating ligands constrain the metals to lie coplanar to a greater extent than those shown in the present series. This coplanar arrangement fosters greater magnetic coupling and accounts for the larger J values. The less constrained adducts of Cu(TSB) with $\mathrm{M(hfa)_2}$ can adopt noncoplanar arrangements, i.e. a bending of the $\mathrm{CuO_1O_2M}$ plane, accounting for the smaller J values.

Ferromagnetism vs. Antiferromagnetism. Another factor that contributes to J is the orbital alignment between the two metals. It has been reported that strict orbital orthogonality, as arises in the Cu(II)–$\mathrm{V^{II}O}$ complexes of 3-formylsalicylic acid, results in ferromagnetism[54] although Selbin and Ganguly[8] reported either antiferromagnetism or no coupling in a series of related Cu(II)–$\mathrm{V^{IV}O}$ Schiff base complexes. The present complexes, Cu(II) with Mn(II), Fe(II), Co(II), and Ni(II), in which there is no orthogonality, are all found to be antiferromagnetic. In addition, it has been observed experimentally[55,56] that orbital orthogonality in a Cu(II)–Fe(III) binuclear (electronically equivalent to the Cu(II)–Mn(II) described here) results in no coupling. This observation is in agreement with predictions from recent calculations,[57] which consider the magnetic interactions via the optimal exchange pathway between Cu(II) and Fe(III) ions. The system has possible spin states $S = 3$ (determinantal wave function $|d_{x^2-y^2,b}d_{xy}d_{xz}d_{yz}d_{z^2}d_{x^2-y^2,a}|$), and $S = 2$ (fourfold degenerate with wave functions $|d_{x^2-y^2,b}{}^2d_{xy}d_{xz}d_{yz}d_{z^2}|$, $|d_{x^2-y^2,b}d_{xy}{}^2d_{xz}d_{yz}d_{z^2}|$, $|d_{x^2-y^2,b}d_{xy}d_{xz}d_{yz}{}^2d_{z^2}|$, $|d_{x^2-y^2,b}d_{xy}d_{xz}{}^2d_{yz}d_{z^2}|$). This leads to an energy difference $E(S{=}3) - E(S{=}2)$, which is positive for all reasonable values of the orbital parameters, predicting antiferromagnetic rather than ferromagnetic coupling in all chemically reasonable Cu–Fe complexes. This is supported by measurements and calculations by Kahn et al.[58] on an antiferromagnetic Fe–Cu complex and a ferromagnetic Cr–Cu complex..

Structure vs. Magnetism. A major challenge is interpreting magnetic exchange properties of a series of heterobinuclear complexes is to deal with all the electronic and structural factors that contribute to J. In the previously described $\mathrm{Cu((prp)_2en)M(hfa)_2}$ series, structural variations outweighed electronic factors in their contributions to J.[6] On the other hand, Hendrickson et al. conclude from the 2,6-dimethyl-4-methylphenol series that the number of d electrons involved is more important than structural variations.[51] However, the latter ligands are relatively rigid, and structural variations are therefore smaller and less important. In the more flexible $\mathrm{Cu(TSB)M(hfa)_2}$ complexes, the structural variations are larger and therefore assume greater importance. Electronic effects are obviously important also, as is evidenced by a steady increase in J as M is varied from Mn to Cu in most series of heterobinuclear complexes, Cu(II)–M(II). Clearly both electronic and structural parameters are important in evaluating magnetic exchange interactions. In a given complex it is possible for either to predominate.

The magnitude of the exchange parameters reported here for the two structurally characterized Cu(II)–Fe(II) ($\mathrm{d^9}$–$\mathrm{d^6}$) systems and the Cu(II)–Mn(II) ($\mathrm{d^9}$–$\mathrm{d^5}$) complex are still somewhat smaller than reported for the Cu(II)–Fe(III) ($\mathrm{d^9}$–$\mathrm{d^5}$) complex in cytochrome *c* oxidase. The magnetic exchange pathway employed by the enzyme must be more closely related to that of the en than the pr complexes, given the weaker coupling in the latter. These results have shown that if the Cu–O–M angles widen and the metals become more coplanar, then J will increase. This indicates that complex **1** is likely to be relatively close to planar in its bridging plane.

Cytochrome Oxidase. The results indicate that in the limit of a planar Cu–Fe system and a favorable Cu–bridge–Fe angle, the magnetic exchange would easily match that reported for the enzyme. This argues in favor of a Cu–O–Fe linkage in the enzyme. The crowded enzyme center would not be able to accommodate more than one bridge. With only one bridge, the Cu–O–Fe angle would tend to open up more to increase the Fe–Cu distance beyond the 2.9 Å in the doubly bridged heterobinuclears. Thus, a distance somewhat above 3 Å is expected. On the other hand, an Im bridge between the metal atoms in heterobinuclears would result in a greater metal–metal separation, but in model complexes, such bridges tend to give smaller magnetic coupling even with optimal bridging geometry.[6,57]

Acknowledgment. Support under NSF Grants CHE83-00516 and CHE83-11449 is gratefully acknowledged.

Registry No. $\mathrm{Cu((prp)_2pr)Ni(hfa)_2}$, 107327-53-7; $\mathrm{Cu((prp)_2pr)Co(hfa)_2}$, 107327-54-8; $\mathrm{Cu((prp)_2pr)Fe(hfa)_2}$, 107327-55-9; $\mathrm{Cu((prp)_2pr)Mn(hfa)_2}$, 107327-56-0; $\mathrm{Cu((prp)_2en)Fe(hfa)_2}$, 107327-57-1; $\mathrm{Cu((prp)_2pr)}$, 107327-58-2; $\mathrm{Cu((prp)_2en)}$, 36820-28-7; $\mathrm{Co(hfa)_2}$, 19648-83-0; $\mathrm{Fe(hfa)_2}$, 28736-68-7; $\mathrm{Mn(hfa)_2}$, 19648-86-3; $\mathrm{Ni(hfa)_2}$, 14949-69-0; cytochrome *c* oxidase, 9001-16-5.

Supplementary Material Available: A packing diagram of $\mathrm{Cu((prp)_2en)Fe(hfa)_2}$ and tables of microanalytical data, thermal parameters, bond lengths and angles, and least-squares planes (23 pages); listings of observed and calculated structure factors (20 pages). Ordering information is given on any current masthead page.

---

(53) Torihara, N.; Okawa, H.; Kida, S. *Chem. Lett.* **1978**, 185.

(54) Kahn, O.; Tola, P.; Galy, J.; Coudanne, H. *J. Am. Chem. Soc.* **1978**, *100*, 3931.

(55) Gunter, M. J.; Mandes, L. N.; McLaughlin, G. M.; Murray, K. S.; Berry, K. J.; Clark, P. E.; Buckingham, D. A. *J. Am. Chem. Soc.* **1980**, *102*, 1470.

(56) Gunter, M. J.; Berry, K. J.; Murray, K. S. *J. Am. Chem. Soc.* **1984**, *106*, 4227.

(57) Brewer, G. A.; Sinn, E., paper presented at the Central/Great Lakes Regional Meeting of the American Chemical Society, Dayton, OH, May 20–22, 1981 (see Abstract INOR 1770); paper presented at the 182nd National Meeting of the American Chemical Society, New York, Aug 23–28, 1981 (see Abstract INOR 297).

(58) Journeaux, Y.; Kahn, O.; Zarembowitch, J.; Galy, J.; Jaud, J. *J. Am. Chem. Soc.* **1983**, *105*, 7585.